

## Test of the transmission line model and the traveling current source model with triggered lightning return strokes at very close range

J. Schoene, M. A. Uman, V. A. Rakov, K. J. Rambo, J. Jerauld, and G. H. Schnetzer  
 Department of Electrical and Computer Engineering, University of Florida, Gainesville, Florida, USA

Received 11 April 2003; revised 7 August 2003; accepted 22 August 2003; published 11 December 2003.

[1] We test the two simplest and most conceptually different return stroke models, the transmission line model (TLM) and the traveling current source model (TCSM), by comparing the first microsecond of model-predicted electric and magnetic field wave forms and field derivative wave forms at 15 m and 30 m with the corresponding measured wave forms from triggered lightning return strokes. In the TLM the return stroke process is modeled as a current wave injected at the base of the lightning channel and propagating upward along the channel with neither attenuation nor dispersion and at an assumed constant speed. In the TCSM the return stroke process is modeled as a current source traveling upward at an assumed constant speed and injecting a current wave into the channel, which then propagates downward at the speed of light and is absorbed at ground without reflection. The electric and magnetic fields were calculated from Maxwell's equations given the measured current or current derivative at the channel base, an assumed return stroke speed, and the temporal and spatial distribution of the channel current specified by the return stroke model. Electric and magnetic fields and their derivatives were measured 15 m and 30 m from rocket-triggered lightning during the summer of 2001 at the International Center for Lightning Research and Testing at Camp Blanding, Florida. We present data from a five-stroke flash, S0105, and compare the measured fields and field derivatives with the model-predicted ones for three assumed lightning return stroke speeds,  $v = 1 \times 10^8$  m/s,  $v = 2 \times 10^8$  m/s, and  $v = 2.99 \times 10^8$  m/s (essentially the speed of light). The results presented show that the TLM works reasonably well in predicting the measured electric and magnetic fields (field derivatives) at 15 m and 30 m if return stroke speeds during the first microsecond are chosen to be between  $1 \times 10^8$  m/s and  $2 \times 10^8$  m/s (near  $2 \times 10^8$  m/s). In general, the TLM works better in predicting the measured field derivatives than in predicting the measured fields. The TCSM does not adequately predict either the measured electric fields or the measured electric and magnetic field derivatives at 15 and 30 m during the first microsecond or so.

*INDEX TERMS:* 3324 Meteorology and Atmospheric Dynamics: Lightning; 0619 Electromagnetics: Electromagnetic theory; 0634 Electromagnetics: Measurement and standards; 3304 Meteorology and Atmospheric Dynamics: Atmospheric electricity; 3367 Meteorology and Atmospheric Dynamics: Theoretical modeling; *KEYWORDS:* lightning, return stroke modeling, modeling

**Citation:** Schoene, J., M. A. Uman, V. A. Rakov, K. J. Rambo, J. Jerauld, and G. H. Schnetzer, Test of the transmission line model and the traveling current source model with triggered lightning return strokes at very close range, *J. Geophys. Res.*, 108(D23), 4737, doi:10.1029/2003JD003683, 2003.

### 1. Introduction and Literature Review

[2] *Rakov and Uman* [1998] have classified a number of frequently used "engineering" return stroke models into two categories, transmission-line-type models and traveling-current-source-type models, with the implied location of the current source and the direction of the current wave as the distinguishing factors. The current source in the transmission-line-type models is often visualized to be at the lightning channel base where it injects an upward-traveling

current wave that propagates behind and at the same speed as the upward-propagating return stroke front. The current source in the traveling-current-source-type models is often visualized as located at the front of the upward-moving return stroke from which point the current injected into the channel propagates downward to ground at the speed of light. Traveling-current-source-type models can also be viewed as involving current sources distributed along the lightning channel that are progressively activated by the upward-moving return stroke front, releasing the charge deposited by the preceding leader [e.g., *Rachidi et al.*, 2002].

[3] The transmission line model (TLM) is the most widely used model of the lightning return stroke and is

the simplest of the models in the transmission-line-type category. The TLM is generally attributed to *Uman and McLain* [1969, 1970], who named and developed it mathematically, although similar models had previously been formulated by *Wagner* [1960] and by *Dennis and Pierce* [1964]. The TLM has been primarily employed to estimate return stroke peak currents and peak current derivatives from measurements of the peak electric field and peak electric field derivative, respectively, with an assumed return stroke speed [e.g., *Weidman and Krider*, 1980; *Krider et al.*, 1996]. These measurements are generally made some tens of kilometers or more from the lightning channel, distances at which the radiation field component of the total electric field dominates the peak value.

[4] In the TLM, the current specified at the base of the channel  $i(0, t)$  is assumed to propagate upward along the channel with a constant speed  $v$ , the speed of the return stroke front. The current at a height  $z'$  from the base of a straight and vertical channel is given by

$$\begin{aligned} i(z', t) &= i(0, t - z'/v) & t \geq z'/v \\ i(z', t) &= 0 & t < z'/v. \end{aligned} \quad (1)$$

[5] The current at a given height  $z'$  is equal to the current at ground at time  $z'/v$  earlier. For a vertical lightning channel over a perfectly conducting flat Earth, *Uman and McLain* [1970] and *Uman et al.* [1975] have shown analytically that, at distances that are much greater than the radiating channel length and for which the radiation field  $E_{\text{rad}}$  is dominant, the TLM predicts the following relationship between the vertical electric field and channel-base current:

$$E_{\text{rad}}(r, t + r/c) = -\frac{v}{2\pi\epsilon_0 c^2 r} i(0, t) \quad (2a)$$

$$E_{\text{rad}} = cB_{\text{rad}}, \quad (2b)$$

where  $B_{\text{rad}}$  denotes the azimuthal magnetic radiation field component,  $r$  is the horizontal distance from the channel base to the observation point,  $c$  is the speed of light, and  $\epsilon_0$  is the permittivity of free space. It is apparent from equation (2a) that if  $v$  is known or assumed and if the distance is known, peak current can be determined from measured electric or magnetic far-field peak, and peak current derivative can be determined from electric or magnetic far-field derivative peak, the latter via the time derivative of (2a).

[6] The Traveling Current Source Model (TCSM), proposed by *Heidler* [1985], is the simplest member of the category of traveling-current-source-type models. In the TCSM the current source is implied to be at the upward-propagating (at constant speed  $v$ ) return stroke front and the current wave propagates downward with the speed of light  $c$  to the Earth where it vanishes (which implies that the channel is terminated in its characteristic impedance). The current at a height  $z'$  from the base of a straight and vertical channel is given by

$$\begin{aligned} i(z', t) &= i(0, t + z'/c) & t \geq z'/v \\ i(z', t) &= 0 & t < z'/v. \end{aligned} \quad (3)$$

The current at a given height  $z'$  is equal to the current at ground at time  $z'/c$  later.

[7] *Willett et al.* [1988, 1989] tested the TLM for return strokes in triggered lightning with electric field and electric field derivative measurements made 5.16 km from the lightning channel. Optical return stroke speeds were also obtained. *Willett et al.* [1989] concluded that

...the TLM provides a reasonable fit to the data for the first one or two  $\mu\text{s}$  of triggered lightning return strokes.  $E_p$  (where  $p$  denotes peak values) is linearly related to  $i_p$  and  $(dE/dt)_p$  to  $(di/dt)_p$ , although the regression line does not pass through the origin and its slope (or the TLM velocity) depends on whether field or field derivative is used.

*Willett et al.* [1989] found, using equation (2a), a TLM mean speed of  $1.6 \times 10^8$  m/s for the field and  $2.0 \times 10^8$  m/s for its derivative. *Willett et al.* [1988, 1989] also argue that if the sharp initial spike observed in their measured electric field wave forms, typically representing about 10% of the peak value, is truncated, the current and electric field wave forms are similar and hence the TLM works better. In order to explain the electric field spike they consider the situation where the junction point of the upward connecting leader from the strike object and the downward dart leader is tens of meters above ground, allowing a downward propagating return stroke component for a short time that contributes to an increase in the overall radiation field for that time. The inferred TLM return stroke speeds are not well correlated with the measured optical speeds but are apparently within the measurement error of the measured optical speeds. For the data of *Willett et al.* [1988], the triggering was done from a 20-m-high, well-grounded structure at the Kennedy Space Center, and, for the data in *Willett et al.* [1989], from a 5 m structure above salt water at the Kennedy Space Center; whereas in the Camp Blanding experiments reported here the strike object was only 2 m high and was located in the center of a  $70 \times 70$  m<sup>2</sup> buried metallic grid, to which it was grounded.

[8] *Thottappillil and Uman* [1993] used the data of *Willett et al.* [1989] to test the TLM, the TCSM, and three other return stroke models. They found that the TLM is "best" for calculating peak currents from measured far-field peaks and measured return stroke speeds because it provides a similar or better result than the other four models from a simpler mathematical relationship (equation (2a)). However, the TLM is not adequate for modeling the fields at later times, after the peak value. For a given current at the channel base, the TCSM and the two other traveling-current-source-type models (the Diendorfer-Uman Model and the Modified Diendorfer-Uman Model, both of which simulate a gradual release of charge into the return stroke channel, as opposed to the TCSM in which the charge is injected into the channel instantaneously at the return stroke front) produced larger electric field peaks than the TL model and another transmission-line-type model (the Modified Transmission Line Model with exponential current decay with height). *Thottappillil and Uman* [1993] noted that a narrow initial spike in some measured electric field wave forms was more likely to be present if the maximum slope of the measured current occurred near the current peak. The initial spikes were reproduced by the traveling-current-source-type models, but not by the transmission-line-type models, although all model-predicted spikes were 1.5 to 10 times larger than the measured spikes. Apparently, the test of the TCSM by *Thottappillil and Uman* [1993] is the only

test of that model using measured fields, currents, and return stroke speeds.

[9] *Leteinturier et al.* [1990] and *Uman et al.* [2000] tested the TLM at the close ranges of 50 m and 10, 14, and 30 m, respectively, using measured peak electric field derivatives and measured peak current derivatives for triggered lightning along with the time derivative of equation (2a). *Leteinturier et al.* [1990] calculated a mean return stroke speed of  $2.9 \times 10^8$  m/s (sample size 40, standard deviation  $4 \times 10^7$  m/s) for the 50 m data. *Uman et al.* [2000] calculated mean return stroke speeds of  $1.7 \times 10^8$  m/s (sample size 7, standard deviation  $5 \times 10^7$  m/s),  $3.1 \times 10^8$  m/s (sample size 3, standard deviation  $1.1 \times 10^8$  m/s), and  $2.9 \times 10^8$  m/s (sample size 7, standard deviation  $7 \times 10^7$  m/s) for the 10 m, 14 m, and 30 m data, respectively. Note that the electric field derivative data at 10 m of *Uman et al.* [2000] may contain errors, as noted by *Schoene et al.* [2003]. The inferred return stroke speeds are likely to be overestimated since the field derivative peak at those close ranges contains, in addition to the radiation component assumed in deriving equation (2a), significant electrostatic and induction components [*Uman et al.*, 2002] (discussed below), a possibility also suggested by *Cooray* [1989] and *Leteinturier et al.* [1990]. In the study of *Leteinturier et al.* [1990], the strike object was the 20-m-high structure at the Kennedy Space Center referred to above, and for the study of *Uman et al.* [2000] it was either a 6-m-high or a 10-m-high structure at Camp Blanding, the site of the experiment discussed in this paper.

[10] *Uman et al.* [2002] used electric and magnetic field derivatives measured at 15 m along with measured current derivatives from triggered lightning to test the TLM. In their experiment, the strike object was a 2 m<sup>2</sup> vertical rod mounted at the center of a 70 × 70 m buried metal grid so as to minimize the effects of the strike object and the effects of field propagation over a poorly conducting Earth. The rocket launcher was placed below the ground surface in a pit. This experimental configuration is the same as that used for acquiring the data reported in the present paper. *Uman et al.* [2002] attempted to reproduce measured field derivatives at 15 m for two strokes (S9934-6 and S9934-7) using the TLM, the expressions for the total electric and magnetic field derivatives (not just radiation field components), and a straight but tilted channel roughly approximating the observed lightning path. The return stroke speed was a variable parameter. *Uman et al.* [2002] calculated the electric and magnetic field derivatives and compared them to the observed field derivatives for speeds of  $1 \times 10^8$ ,  $2 \times 10^8$ , and  $2.99 \times 10^8$  m/s and found that a reasonable match, given the potential measurement errors, was achieved for both strokes for a return stroke speed between  $2 \times 10^8$  m/s and  $2.99 \times 10^8$  m/s. Their calculations showed that all electric field components (electrostatic, induction, and radiation) are significantly present in the electric field derivative peaks at 15 m and 30 m for a speed of  $2 \times 10^8$  m/s and that, while the derivative wave shape does not change significantly from 15 m to 30 m, the mix of electric field components does. Note that *Thottappillil and Rakov* [2001] have shown that the separation of the total electric field into the three components noted above is not unique.

[11] In this paper, we study triggered lightning strokes that exhibited straight and nearly vertical channels to test

the adequacy of both the TLM and the TCSM. We present measured electric and magnetic fields and their derivatives and compare them with those calculated using the two models, whose inputs are measured channel-base current and current derivative and three assumed return stroke speeds:  $1 \times 10^8$ ,  $2 \times 10^8$ , and  $2.99 \times 10^8$  m/s. We show that the TLM provides a reasonable fit to the measured data for the first microsecond while the TCSM does not.

## 2. Experiment and Data

[12] The experiment was conducted in 2001 at the International Center for Lightning Research and Testing (ICLRT) at Camp Blanding in north central Florida. The 2001 experiment was similar to the 1999 and 2000 experiments which have been described briefly in the previous section and in detail by *Crawford et al.* [2001], *Rakov et al.* [2001], *Miki et al.* [2002], *Uman et al.* [2002], and *Schoene et al.* [2003]. A sketch of the arrangement of sensors during 1999, 2000, and 2001 at the ICLRT is given in Figure 1. A photograph showing the strike object, a 2 m rod projecting above a metal mesh ground plane, the pit housing the underground launcher, and triggered lightning event S0105 from summer 2001, analyzed here, is found in Figure 2.

[13] We measured currents and current derivatives at the lightning channel base as well as the electric and magnetic fields and their time derivatives at distances of 15 m and 30 m from the strike point. All data were low-pass filtered before they were digitized with sampling rates ranging from 25 MHz to 250 MHz. The measured parameters with the corresponding 3 dB cutoff frequency of the low-pass filter and the sampling rate are listed in Table 1.

[14] We tested the accuracy of the measured parameters for the strokes of lightning flash S0105 by comparing the measured current derivatives and the measured electric and magnetic field derivatives with the corresponding numerically differentiated currents and fields. We use the current and the field derivatives for this test rather than the currents and fields because the derivative wave forms provide a more sensitive measure of comparison. The measured  $dl/dt$  wave forms and the differentiated current wave forms are generally in good agreement (ratio of peaks of measured wave forms/peaks of numerically differentiated wave forms mean: 0.95, standard deviation: 0.07). The  $dE/dt$  wave forms measured at distances of 15 m and 30 m are on average larger than the differentiated electric field wave forms (mean ratio of peaks: 1.17, standard deviation: 0.22). The  $dB/dt$  wave forms measured at distances of 15 m and 30 m are on average similar to the differentiated magnetic field wave forms, although there is considerable dispersion in the ratio of the peaks (ratio of peaks mean: 0.96, standard deviation: 0.21). Note that the measured  $dB/dt$  at 15 m for stroke 5 and the measured  $dE/dt$  at 30 m for strokes 3, 4, and 5 are slightly clipped and consequently the maximum value, mean, and standard deviation in the statistics above that include these underestimated parameters are also slightly underestimated. Further, note that the fields and field derivatives are measured in different locations (Figure 1). Note also that the shapes of the differentiated wave forms are generally wider than the shapes of the measured derivative wave forms. The discrepancies between the directly measured derivatives and those obtained

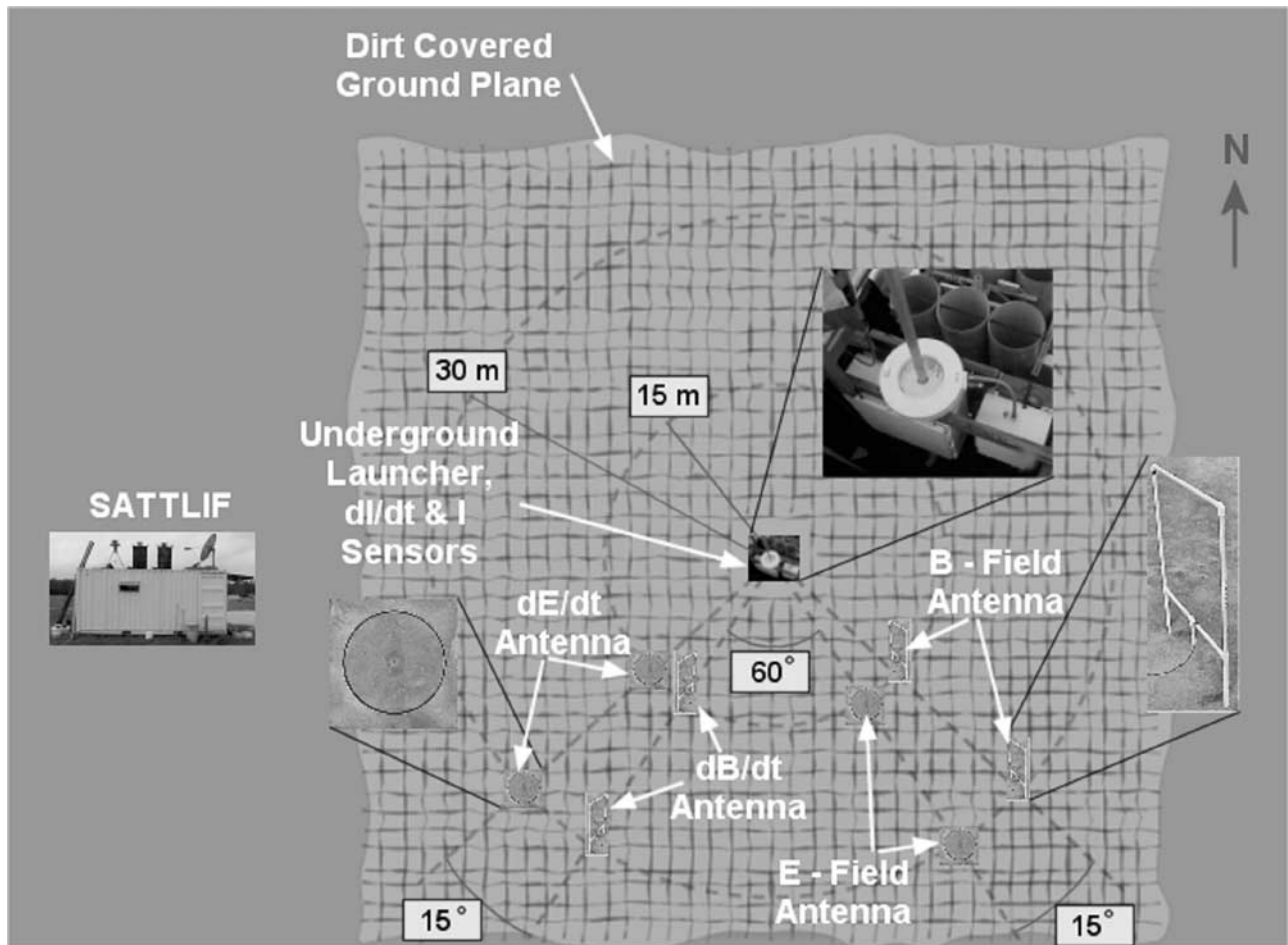


**Figure 1.** Underground launcher with the strike rod and current and current derivative measuring devices in the center of the buried metal grid and with electric ( $E$ ) and magnetic ( $B$ ) field and field derivative ( $dE/dt$  and  $dB/dt$ ) antennas at 15 m and 30 m.

by numerical differentiation can in part be attributed to the different locations of the field and field derivative measurements from lightning channels that are not exactly vertical or straight, in part to the considerable bit noise that is present in all numerically differentiated wave forms, and possibly to the poorer frequency response or insufficient sampling rate of the field measurements.

### 3. Theory

[15] The vertical electric field intensity ( $E_z$ ) and the azimuthal magnetic flux density ( $B_\phi$ ) of a lightning return stroke at ground level at a horizontal distance  $r$  from the bottom of a vertical lightning channel over a perfectly conducting ground are [Thottappillil *et al.*, 1997]

$$\begin{aligned}
 E_z(r, t) = & \frac{1}{2\pi\epsilon_0} \int_0^{L(t)} \left( \frac{2z'^2 - r^2}{R^5(z')} \right) \int_{t_b(z')}^t i(z', \tau - R(z')/c) d\tau \\
 & + \frac{2z'^2 - r^2}{cR^4(z')} i(z', t - R(z')/c) \\
 & - \frac{r^2}{c^2R^3(z')} \frac{\partial i(z', t - R(z')/c)}{\partial t} dz' \\
 & - \frac{1}{2\pi\epsilon_0} \frac{r^2}{c^2R^3(L(t))} i(L(t), L(t)/v) \frac{dL(t)}{dt}
 \end{aligned} \tag{4}$$



**Figure 2.** A photograph of the experimental site and triggered lightning S0105. The photograph was taken from the SATTLIF trailer (see Figure 1). The two vertical objects on either side of the strike rod are shock wave sensors, not shown in Figure 1.

**Table 1.** 3 dB Cutoff Frequencies of the Low-Pass Filters and Sampling Rates of the Measurements for Lightning Flash S0105

	Current		Electric Field		Electric Field Derivative		Magnetic Field		Magnetic Field Derivative	
	Current	Derivative	15 m	30 m	15 m	30 m	15 m	30 m	15 m	30 m
3 dB cutoff frequency, MHz	20	20	10	20	20	20	10	10	20	20
Sampling rate, MHz	25	250	25	25	250	250	50	50	250	50

$$\begin{aligned}
B_{\phi}(r, t) = & \frac{\mu_0}{2\pi} \int_0^{L(t)} \left( \frac{r}{R^3(z')} i(z', t - R(z')/c) \right. \\
& + \frac{r}{cR^2(z')} \frac{\partial i(z', t - R(z')/c)}{\partial t} \Big) dz' \\
& + \frac{\mu_0}{2\pi} \frac{r}{cR^2(L(t))} i(L(t), L(t)/v) \frac{dL(t)}{dt}, \quad (5)
\end{aligned}$$

where  $\epsilon_0$  is the permittivity and  $\mu_0$  the permeability of free space,  $c$  is the speed of light,  $t_b$  is the time at which the current at  $z'$  is first “seen” by the observer,  $v$  is the return stroke speed,  $L(t)$  is the radiating length of the channel, and  $R$  is the distance between the current carrying channel segment  $dz'$  and the observation point on ground. The first three terms in equation (4) are known as the electrostatic, induction, and radiation components of the electric field, respectively. The first two terms in equation (5) are commonly referred to as the induction (or magnetostatic) and radiation components of the magnetic field, respectively. The last term in equations (4) and (5) is an additional radiation field component that accounts for any discontinuity at the upward moving return stroke front, such a discontinuity being an inherent feature of the TCSM. The electric and magnetic fields can be calculated from equations (4) and (5), respectively, once the current distribution (or equivalently the charge density distribution) along the channel is specified according to the return stroke model. Return stroke models formulated in terms of the charge density distribution can allow a deeper insight into the physical processes of the return stroke. *Thottappillil et al.* [1997] applied the continuity equation to relate the current and the charge density distributions along the lightning channel for various return stroke models and decomposed the total charge density distribution into two components: (1) A component that is nonzero only during the return stroke process and is zero after the return stroke current ceases to flow in the channel. This component can be viewed as the charge per unit length transferred through the channel. (2) A component that is nonzero both during and after the return stroke process. This component can be interpreted as the charge per unit length deposited by the return stroke on the channel. The interpretation of the two charge density components is also discussed by *Rakov et al.* [2003].

[16] The line charge density along the channel for the TLM, given by *Thottappillil et al.* [1997], is

$$\rho_L(z', t) = \frac{i(0, t - z'/v)}{v}. \quad (6)$$

Equation (6) becomes zero after the return stroke process ends. It follows that the TLM only allows transferred charge

through the channel and no net charge is deposited onto (or removed from) the channel.

[17] The line charge density along the channel for the TCSM, given by *Thottappillil et al.* [1997], is

$$\rho_L(z', t) = -\frac{i(0, t + z'/c)}{c} + \frac{i(0, z'/v^*)}{v^*}, \quad (7)$$

where  $v^* = v/(1 + v/c)$ . The first term is associated with the downward moving current wave and represents the transferred charge. The second term is due to the upward moving front and represents the return stroke charge deposited on the channel (or leader charge removed from the channel). For the charge density at ground ( $z' = 0$ ), if there is no discontinuity at  $t = 0$  in the channel-base current, the second term in equation (7) is equal to zero ( $i(0, 0)/v^* = 0$ ) and the total charge density becomes

$$\rho_L(0, t) = -\frac{i(0, t)}{c}. \quad (8)$$

[18] The charge density at the front ( $t = z'/v$ ) is

$$\rho_L(z', z'/v) = \frac{i(0, z'/v^*)}{v}, \quad (9)$$

as shown by *Thottappillil et al.* [1997]. Note that the charge density distribution along the channel is bipolar since equation (8) for the charge density at ground is negative (if  $i(0, 0)/v^* = 0$ ) and equation (9) for the charge density at the front is always positive. *Thottappillil et al.* [1997] attributed the presence of the negative charge at the channel bottom to the fact that the TCSM implicitly assumes that the channel is terminated in its characteristic impedance, that is, the current reflection coefficient at ground is zero. In most cases this assumption is invalid since the impedance of the lightning channel is typically much larger than the impedance of the grounding, resulting in a current reflection coefficient close to one (short circuit conditions at ground). Under short circuit conditions,  $\rho_L(0, t) = 0$  at all times, as opposed to a negative value according to equation (8). Modifications to the TCSM attempting to account for current reflections at ground are found in the work of *Heidler and Hopf* [1994, 1995].

#### 4. Modeling Results

[19] Vertical electric fields and azimuthal magnetic fields and their time derivatives at ground level at two distances, 15 m and 30 m, are calculated for all 5 strokes of flash S0105 using both the TLM and the TCSM. The measured currents and the measured current derivatives shown in

Figure 3, along with three assumed return stroke speeds,  $v_1 = 1 \times 10^8$  m/s,  $v_2 = 2 \times 10^8$  m/s, and  $v_3 = 2.99 \times 10^8$  m/s (essentially the speed of light  $c$ ), are used as inputs to equations (4) and (5) for the field calculation and the derivatives of equations (4) and (5) for the field derivative calculation, respectively. That is, measured current and its numerically evaluated integral and derivative are used in the field calculation, while measured current derivative and numerically evaluated functions of that derivative are used in the field derivative calculation. Both measured current and measured current derivative are best not used in a single calculation because they cannot be exactly aligned in time. In Figure 4, the modeling results are compared with the corresponding measured fields and field derivatives.

[20] The comparison shows that the TLM generally works well in predicting the electric and magnetic fields if speeds between  $1 \times 10^8$  m/s and  $2 \times 10^8$  m/s are used; the exceptions being the electric fields at 15 m and 30 m for stroke 5 (all modeled electric fields are larger than the measured fields).

[21] The TCSM typically produces a narrow spike in the rising portion of the electric and magnetic field wave forms which is not present in the measured fields. This spike, whose duration is of the order of 100 ns, is more pronounced for larger return stroke speeds, that is  $v = 2 \times 10^8$  m/s and  $v = 2.99 \times 10^8$  m/s. The TCSM therefore fails to reproduce adequately the front of the electric and magnetic field wave forms, particularly if large return stroke speeds are used. The model-predicted electric field wave forms after the initial peak are generally in good agreement with the measured fields if speeds of about  $1 \times 10^8$  m/s or lower (modeling result for lower speeds are available but are not shown here) are used and are much lower than the measured field wave forms if the electric fields are computed using  $v = 2 \times 10^8$  m/s and  $v = 2.99 \times 10^8$  m/s. The model-predicted magnetic field wave forms after the initial peak are in good agreement with the measured magnetic fields for all three speeds considered here.

[22] The TLM works very well in predicting the electric and magnetic field derivatives if speeds near  $2 \times 10^8$  m/s are used. Again, the exceptions are the electric field derivatives at 15 m and 30 m for stroke 5 (all modeled electric field derivatives are larger than the measured ones).

[23] The TCSM yields electric and magnetic field derivative peaks that are much larger and sharper than the corresponding measured peaks, followed by peaks of opposite polarity that are not observed in the measured derivative wave forms (these bipolar signatures in the field derivatives are related to the initial narrow spike in the TCSM fields). Therefore the TCSM fails to reproduce adequately measured electric and magnetic field derivative wave forms at 15 and 30 m.

## 5. Discussion

[24] The TCSM produces narrow spikes in the electric and magnetic fields and bipolar signatures in the electric and magnetic field derivatives, features not observed in the measured fields and field derivatives at 15 and 30 m presented here. Also, the TCSM underestimates the measured electric fields after the maximum for the higher assumed return stroke speeds ( $v = 2 \times 10^8$  m/s and  $v =$

$2.99 \times 10^8$  m/s). In order to understand better the TCSM and the differences between the two models studied here, we calculated the line charge density versus time by applying the TLM and the TCSM (equations (6) and (7)) for return stroke 1 with three return stroke speeds ( $v = 1 \times 10^8$  m/s,  $v = 2 \times 10^8$  m/s, and  $v = 2.99 \times 10^8$  m/s). The results, presented in Figure 5, show that for the TLM the return stroke charge density is always positive while for the TCSM the return stroke charge density distribution along the channel is bipolar, as previously pointed out by *Thottappillil et al.* [1997] and *Rakov et al.* [2003] and discussed here following equation (9). Note that for the TCSM, the larger the speed, the longer the portion of the channel that is negatively charged: for  $v = 1 \times 10^8$  m/s,  $v = 2 \times 10^8$  m/s, and  $v = 2.99 \times 10^8$  m/s, the bottom 10 m, 25 m, and 40 m, respectively, of the lightning channel are negatively charged. Since the TCSM does not match the experimental data for the larger speeds, as discussed above, the deficiencies in the model, i.e., the spikes in the electric and magnetic fields and the underestimation of the electric fields after the maximum, might be related to the unexpected presence of the negative charge on the bottom section of the channel, that section being longer for larger speeds. Note that the applicability of the TCSM also appears to depend on the shape of the initial rising portion of the channel-base current, that is, the deficiencies in the TCSM are more pronounced (and a longer portion of the channel is negatively charged) when the maximum current slope occurs closer to the current peak, a modeling result for which no figure is shown in this paper. The latter effect was previously considered by *Thottappillil and Uman* [1993].

[25] *Willett et al.* [1988, 1989] observed narrow electric field spikes in their distant (5.16 km) electric field data measured at the Kennedy Space Center (KSC) in 1985 and 1987 (see our section 1). *Thottappillil and Uman* [1993] calculated electric fields at 5.16 km using various return stroke models, with model inputs being the channel-base current measured during the 1987 KSC experiment and the optically measured return stroke speeds. They found that the TCSM-predicted electric fields contain spikes similar to those observed in the measured fields. It is, however, unlikely that the TCSM-predicted distant (radiation) electric field spikes reported by *Thottappillil and Uman* [1993] and the distant electric field spikes in the data of *Willett et al.* [1988, 1989] are associated with the same physical processes, since the TCSM also predicts spikes in the close electric fields which are not present in our measured electric fields at distances of 15 m and 30 m. It thus appears more likely that the electric field spikes in the 5.16 km KSC data are related to an initial bidirectional extension of the return stroke channel originating from the junction point of the downward and the upward-connecting leaders and involving propagation down the upward leader and the strike object with reflections at the top of the object and at ground [e.g., *Rachidi et al.*, 2002]. Such a bidirectional return stroke process has been considered by *Wagner and Hileman* [1958], *Uman et al.* [1973], *Weidman and Krider* [1978], *Willett et al.* [1988, 1989], and *Leteinturier et al.* [1990] and has been documented by *Wang et al.* [1999].

[26] The electric field spikes observed by *Willett et al.* [1988] (1985 data, a 20-m-high strike object) had a mean magnitude that was about 11% of the total electric field peak

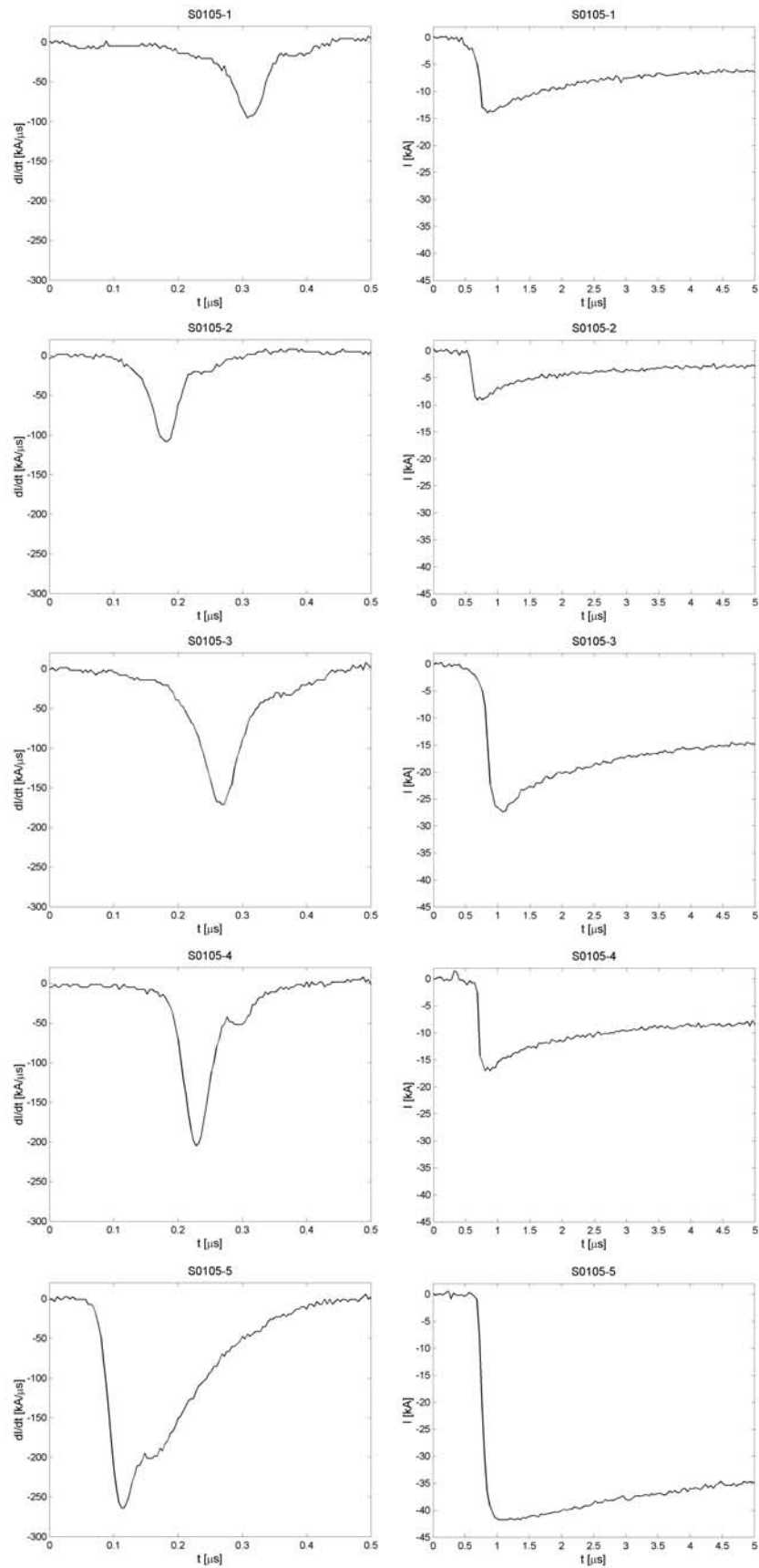


**Figure 3.** Measured (left) current derivatives and (right) currents of five return strokes in flash S0105. Current derivatives are shown on a  $0.5\text{-}\mu\text{s}$  timescale, and currents are shown on a  $5\text{-}\mu\text{s}$  timescale.

a) Flash S0105, Return Stroke 1

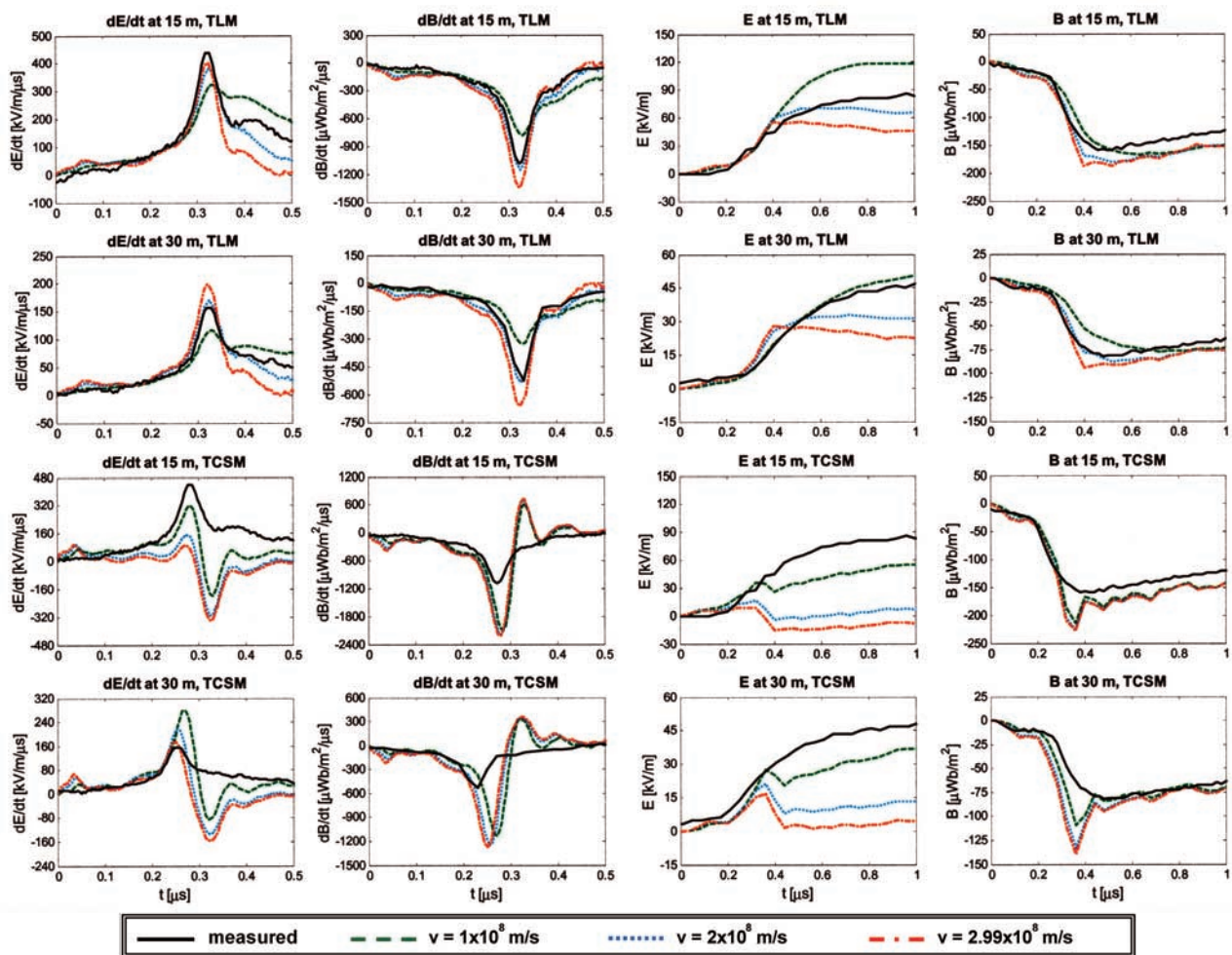


**Figure 4.** Measured electric/magnetic field derivatives (first/second columns) and electric/magnetic fields (third/fourth columns) at 15 m and 30 m for flash S0105, (a–e) strokes 1–5 overlaid with the corresponding model-predicted fields and field derivatives using the TLM/TCSM (first and second rows/ third and fourth rows), and  $v = 1 \times 10^8$ ,  $2 \times 10^8$ , and  $2.99 \times 10^8$  m/s. The field derivatives/fields are shown on a 0.5/1  $\mu$ s time window. Note that the vertical scales of the graphs vary according to the vertical ranges of variation of the displayed wave forms. Some measured wave forms do not begin at near-zero amplitude but at the finite value of the dart leader field prior to return stroke initiation.

and the mean magnitudes of the spikes measured by *Willett et al.* [1989] (1987 data, a 5-m-high strike object) were about 5% of the total electric field peak. Considering that the length of the upward going leader is expected to be greater for taller strike objects due to the greater electric field enhancement by taller objects and assuming that larger magnitudes of the electric field spikes are associated with taller strike objects having longer upward going leaders, the presence of larger spikes in the 1985 data (20-m-high strike object) compared to the spikes in the 1987 KSC data (5-m-high strike object) may be viewed as supporting the hypothesis that the spikes are due to an initial bidirectional extension of the return stroke channel involving return stroke propagation down both the upward leader and the strike object as well as up the downward leader channel.

[27] The measured and model-predicted electric and magnetic field derivatives presented here attain peak value 100

to 300 ns after return stroke initiation, and the electric and magnetic fields flatten or reach peak value 400 ns to 1  $\mu$ s after initiation (flattening of very close return stroke electric field wave forms within 15  $\mu$ s or so is considered to be a characteristic feature of these wave forms [e.g., *Rakov and Uman*, 1998]). It follows that the field derivatives are likely associated with features of the return stroke process occurring at early times, while the fields are more closely related to the return stroke process at later times when the field derivatives are relatively small. Some speculation related to this observation are found in the next two paragraphs.

[28] The TLM reproduces the measured field derivatives well for return stroke speeds near  $2 \times 10^8$  m/s and reproduces the measured fields well for lower return stroke speeds (between  $1 \times 10^8$  m/s and  $2 \times 10^8$  m/s). This observation could be interpreted to indicate that the return stroke speed in the bottom tens of meters of the channel



## b) Flash S0105, Return Stroke 2

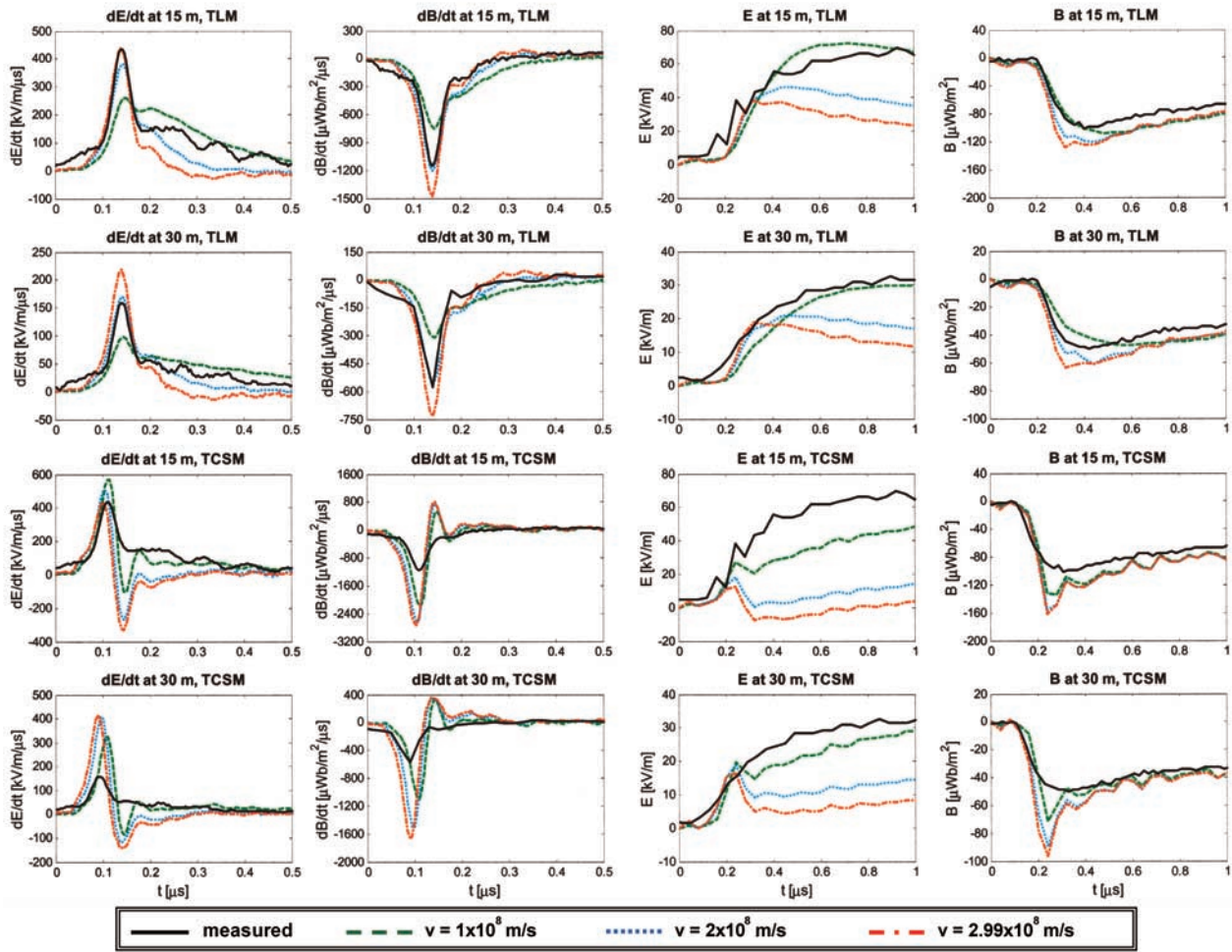


Figure 4. (continued)

decreases rapidly with height, although, strictly speaking, the model is not valid for a time-varying return stroke speed. Also, the bottom 10 m or so may involve an upward connecting leader [Wang *et al.*, 1999], not considered in the model.

[29] For strokes 1, 2, 3, and 4, the TLM with a return stroke speed close to  $2 \times 10^8$  m/s gives the best overall match between measured and model-predicted electric and magnetic field derivatives. A speed that gives the best overall match for the electric fields of these four strokes cannot be found. One of the possible, admittedly speculative, interpretations of this result is that there is less variation in return stroke speeds between strokes at early times when the return stroke front is within some tens of meters of the channel bottom than there is for return stroke speeds at later times. Again, strictly speaking, the model does not allow this inference.

[30] There are various modification of the TLM that allow a current decay with height and hence a deposited charge on the channel (e.g., the modified transmission line model with linear current decay with height [Rakov and Dulzon, 1987] and the modified transmission line model with exponential current decay with height [Nucci *et al.*,

1988]). For the first  $1 \mu\text{s}$  of the return stroke modeled in the present paper, the results obtained here are essentially the same as would be obtained during the first  $1 \mu\text{s}$  using those modified TL-type models since the current versus height profile is essentially the same for the different TL-type models for the first microsecond. As noted in section 3, the TCSM can be modified to take account of current reflections at ground. Potentially, this modification might alter the bipolar nature of the TCSM charge distribution discussed above and in section 3 with the resultant TCSM wave forms being possibly different from those presented here.

## 6. Concluding Remarks

[31] The TLM works reasonably well in reproducing close measured electric and magnetic fields if return stroke speeds during the first microsecond are chosen to be between  $1 \times 10^8$  m/s and  $2 \times 10^8$  m/s, and works well in reproducing field derivatives for return stroke speeds near  $2 \times 10^8$  m/s. This result is very similar to that of Willett *et al.* [1989] (see section 1) obtained from measurements of radiation (far) fields at 5.16 km whereas the present estimation of return stroke speed involves close field wave

c) Flash S0105, Return Stroke 3

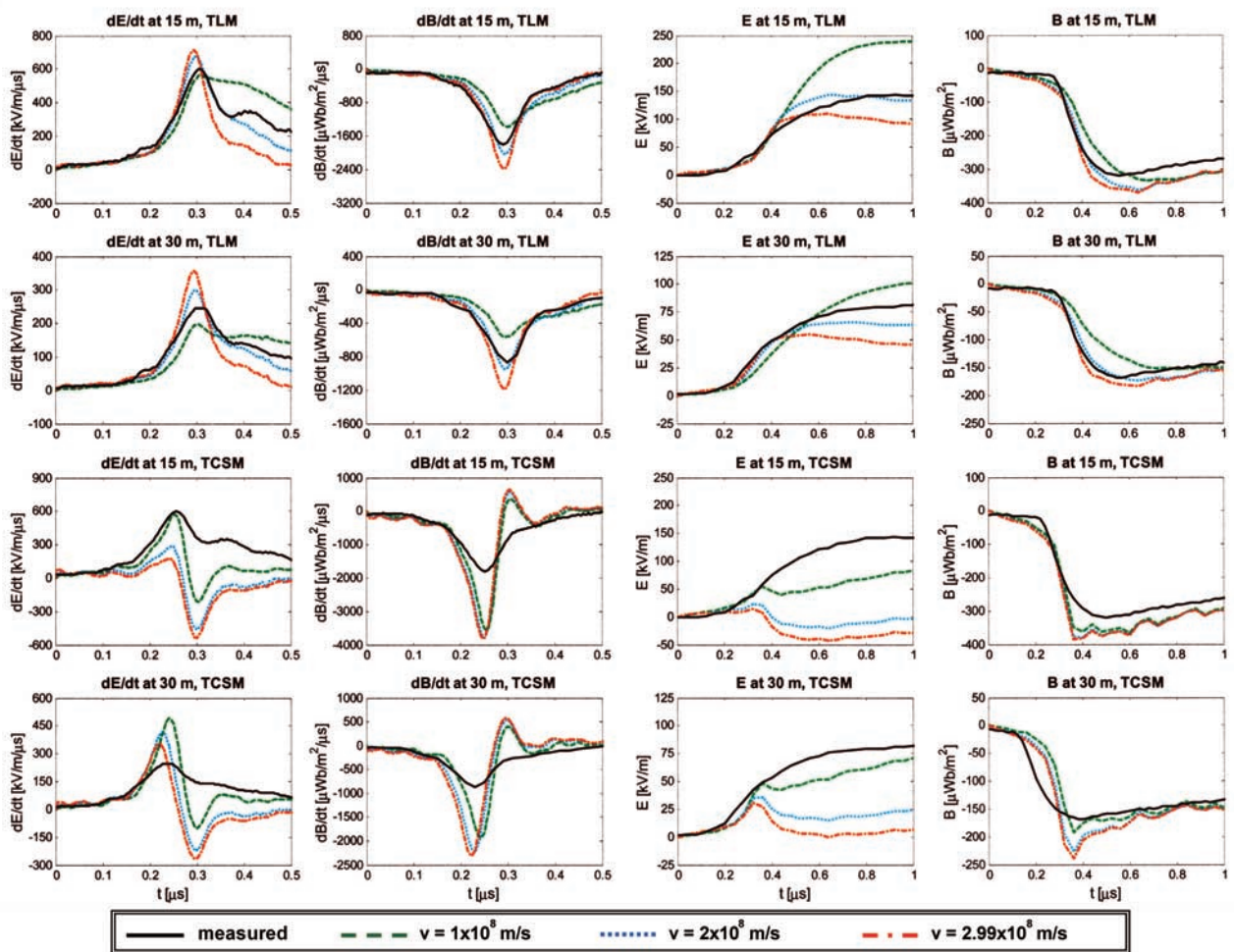


Figure 4. (continued)

d) Flash S0105, Return Stroke 4

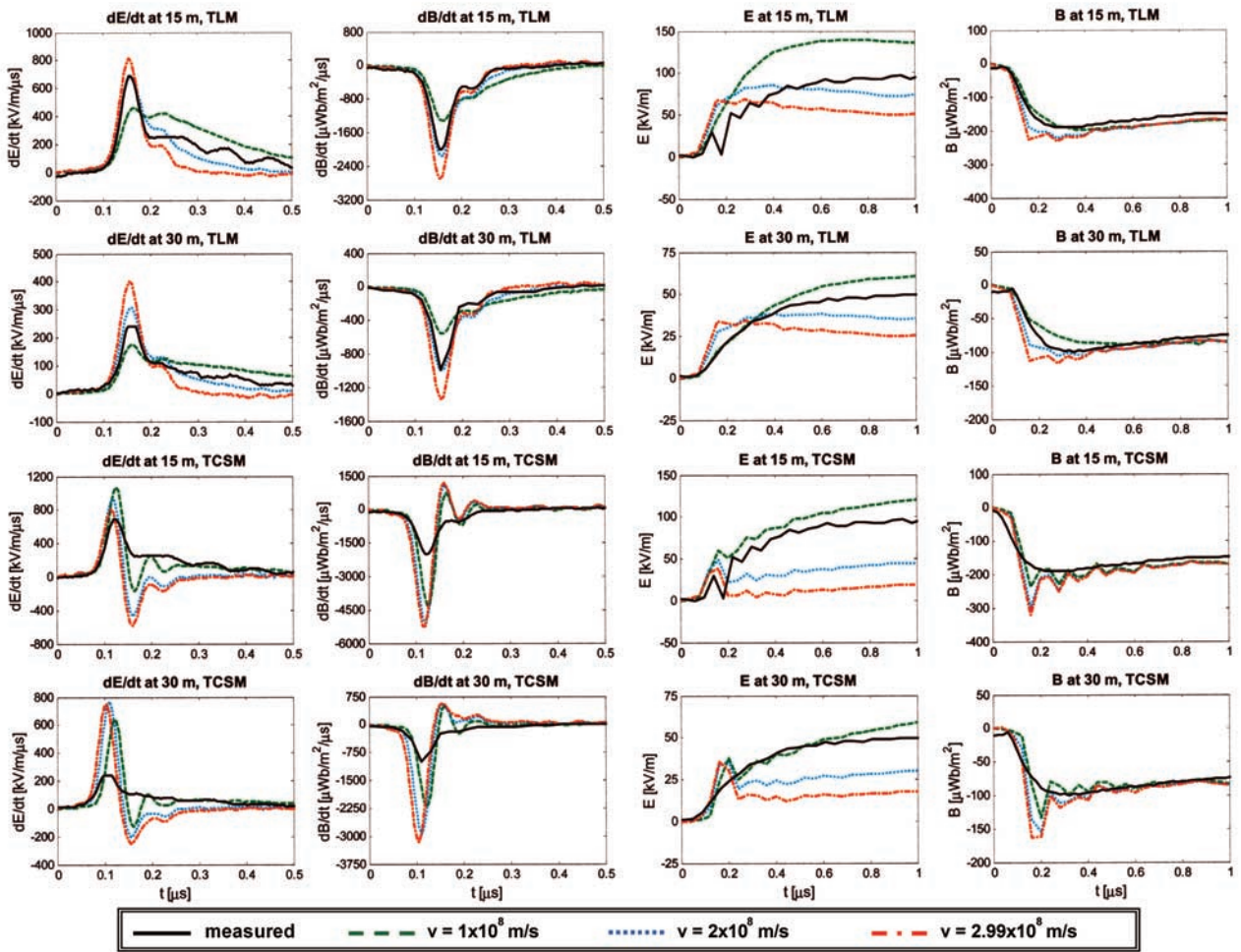


Figure 4. (continued)

e) Flash S0105, Return Stroke 5

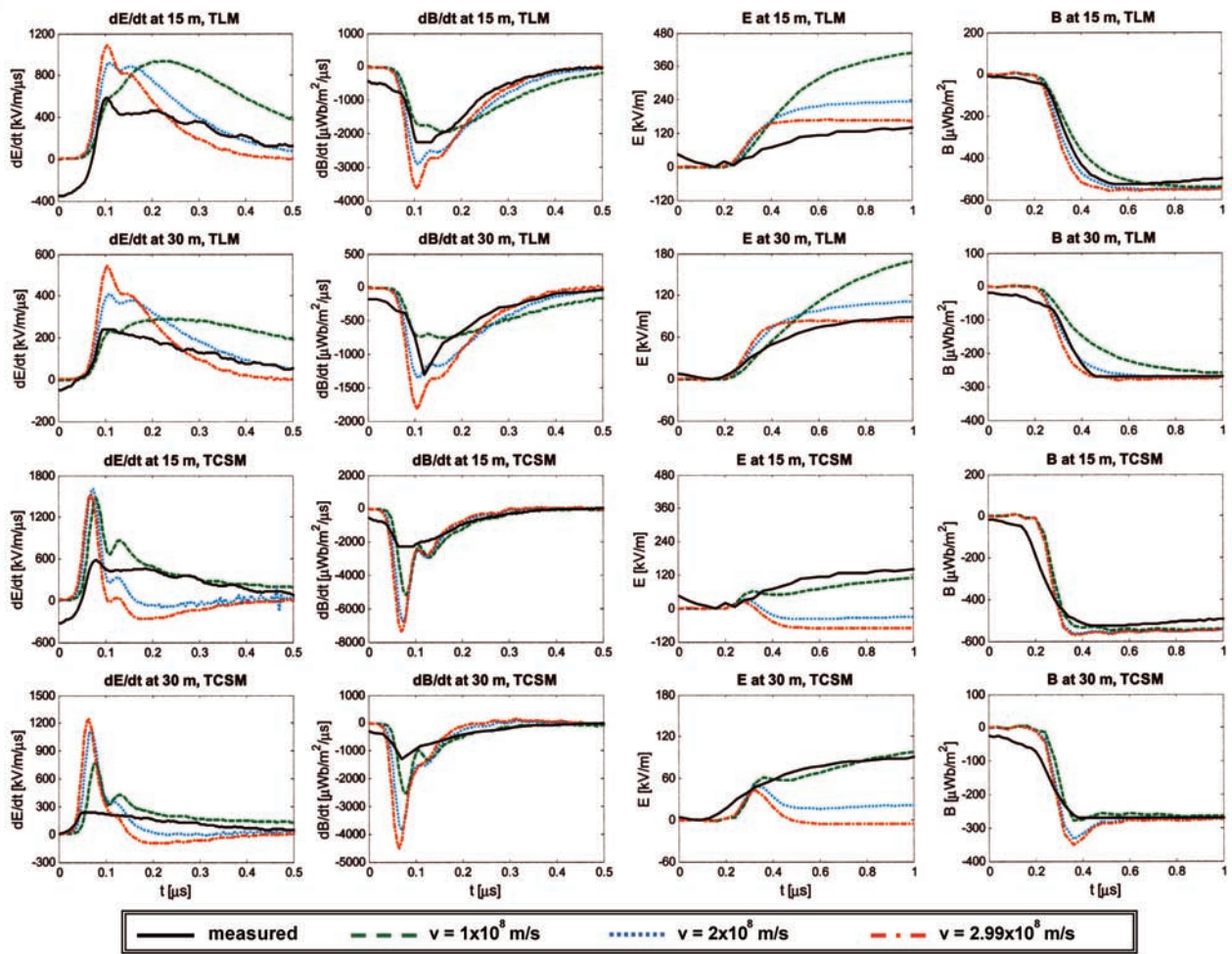
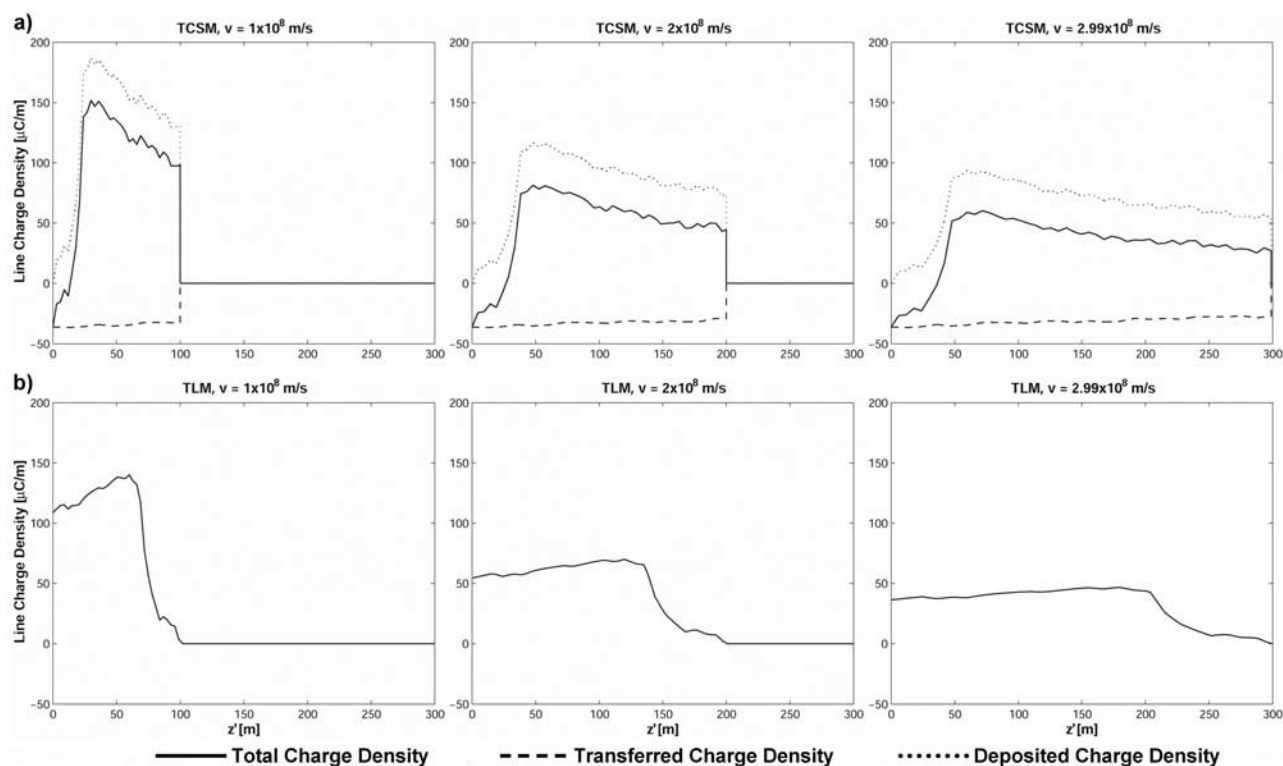


Figure 4. (continued)



**Figure 5.** Line charge densities associated with the return stroke process versus channel height  $z'$  above ground at  $1 \mu\text{s}$  for stroke 1 of flash S0105 calculated using (a) the TCSM and (b) the TLM. Note that for the TLM the total charge density is equal to the transferred charge density. Note that the total return stroke charge density distribution for the TLM is unipolar, while for the TCSM it is bipolar.

forms (at 15 and 30 m) that contain significant, if not dominant, near-field components [Uman et al., 2002]. The TCSM is deficient in modeling the 15 and 30 m fields, probably because it predicts a negative charge density at and near the channel bottom that is apparently related to the unrealistic assumption of matched conditions at the ground for the downward propagating current wave, while short circuit conditions are expected in most practical situations. The effect is more pronounced for higher return stroke speeds and for current wave forms with a maximum current rate of rise close to the current peak. Modifications to the TCSM related to the channel termination on ground should be considered to determine if such modification would improve the agreement with measurements. Further, other traveling current source type models such as the Diendorfer-Uman model [Diendorfer and Uman, 1990] should be tested against experimental data. Such additional modeling will be the subject of a future paper.

[32] **Acknowledgments.** This research was supported in part by DOT (FAA) Grant 99-G-043 and NSF Grant ATM-0003994.

## References

- Cooray, V., Derivation of return stroke parameters from the electric and magnetic field derivatives, *Geophys. Res. Lett.*, 16, 61–64, 1989.
- Crawford, D. E., V. A. Rakov, M. A. Uman, G. H. Schnetzer, K. J. Rambo, M. V. Stapleton, and R. J. Fisher, The close lightning electromagnetic environment: Dart-leader electric field change versus distance, *J. Geophys. Res.*, 106, 14,909–14,917, 2001.
- Dennis, A. S., and E. T. Pierce, The return stroke of the lightning flash to Earth as a source of VLF atmospherics, *Radio Sci.*, 68D, 777–794, 1964.
- Diendorfer, G., and M. A. Uman, An improved return stroke model with specified channel-based current, *J. Geophys. Res.*, 95, 13,621–13,644, 1990.
- Heidler, F., Traveling current source model for LEMP calculation, paper presented at the 6th International Symposium on Electromagnetic Compatibility, Swiss Fed. Inst. of Technol., Zurich, Switzerland, March 1985.
- Heidler, F., and C. Hopf, Lightning current and lightning electromagnetic impulse considering current reflection at the Earth's surface, paper presented at the 22nd International Conference on Lightning Protection, paper R 4-05, Tech. Univ. of Budapest, Budapest, Hungary, 1994.
- Heidler, F., and C. Hopf, Influence of channel-base current and current reflections on the initial and subsidiary lightning electromagnetic field peak, paper presented at the International Aerospace and Ground Conference on Lightning and Static Electricity, Natl. Interagency Coord. Group, Williamsburg, Va., 1995.
- Krider, E. P., C. Leteinturier, and J. C. Willett, Submicrosecond fields radiated during the onset of first return strokes in cloud-to-ground lightning, *J. Geophys. Res.*, 101, 1589–1597, 1996.
- Leteinturier, C., C. Weidman, and J. Hamelin, Current and electric field derivatives in triggered lightning return strokes, *J. Geophys. Res.*, 95, 811–828, 1990.
- Miki, M., V. A. Rakov, K. J. Rambo, G. H. Schnetzer, and M. A. Uman, Electric fields near triggered lightning channels measured with Pockels sensors, *J. Geophys. Res.*, 107(D16), 4277, doi:10.1029/2001JD001087, 2002.
- Nucci, C. A., C. Mazzetti, F. Rachidi, and M. Ianoz, On lightning return stroke models for LEMP calculations, paper presented at the 19th International Conference on Lightning Protection, ÖVE, Graz, Austria, April 1988.
- Rachidi, F., V. A. Rakov, C. A. Nucci, and J. L. Bermudez, The effect of vertically extended strike object on the distribution of current along the lightning channel, *J. Geophys. Res.*, 107(D23), 4699, doi:10.1029/2002JD002119, 2002.
- Rakov, V. A., and A. A. Dulzon, Calculated electromagnetic fields of lightning return stroke, *Tekh. Elektrodinam.*, 1, 87–89, 1987.
- Rakov, V. A., and M. A. Uman, Review and evaluation of lightning return stroke models including some aspects of their application, *IEEE Trans. Electromagn. Compat.*, 40, 403–426, 1998.

- Rakov, V. A., D. E. Crawford, K. J. Rambo, G. H. Schnetzer, M. A. Uman, and R. Thottappillil, M-component mode of charge transfer to ground in lightning discharges, *J. Geophys. Res.*, *106*, 22,817–22,831, 2001.
- Rakov, V. A., R. Thottappillil, and J. Schoene, Comments on “On the *IEEE Trans Electromagn. Compat.*, concepts used in return stroke models applied in engineering practice,” *45*, 567, 2003.
- Schoene, J., M. A. Uman, V. A. Rakov, V. Kodali, K. J. Rambo, and G. H. Schnetzer, Statistical characteristics of the electric and magnetic fields and their time derivatives 15 m and 30 m from triggered lightning, *J. Geophys. Res.*, *108*(D6), 4192, doi:10.1029/2002JD002698, 2003.
- Thottappillil, R., and V. A. Rakov, On different approaches to calculating lightning electric fields, *J. Geophys. Res.*, *106*, 14,191–14,205, 2001.
- Thottappillil, R., and M. A. Uman, Comparison of lightning return-stroke models, *J. Geophys. Res.*, *98*, 22,903–22,914, 1993.
- Thottappillil, R., V. A. Rakov, and M. A. Uman, Distribution of charge along the lightning channel: Relation to remote electric and magnetic fields and to return-stroke models, *J. Geophys. Res.*, *102*, 6987–7006, 1997.
- Uman, M. A., and D. K. McLain, Magnetic field of lightning return stroke, *J. Geophys. Res.*, *74*, 6899–6910, 1969.
- Uman, M. A., and D. K. McLain, Lightning return stroke current from magnetic and radiation field measurements, *J. Geophys. Res.*, *75*, 5143–5147, 1970.
- Uman, M. A., D. K. McLain, R. J. Fisher, and E. P. Krider, Currents in Florida lightning return strokes, *J. Geophys. Res.*, *78*, 3530–3537, 1973.
- Uman, M. A., D. K. McLain, and E. P. Krider, The electromagnetic radiation from a finite antenna, *Am. J. Phys.*, *43*, 33–38, 1975.
- Uman, M. A., V. A. Rakov, G. H. Schnetzer, K. J. Rambo, D. E. Crawford, and R. J. Fisher, Time derivative of the electric field 10, 14, and 30 m from triggered lightning strokes, *J. Geophys. Res.*, *105*, 15,577–15,595, 2000.
- Uman, M. A., J. Schoene, V. A. Rakov, K. J. Rambo, and G. H. Schnetzer, Correlated time derivatives of current, electric field intensity, and magnetic flux density for triggered lightning at 15 m, *J. Geophys. Res.*, *107*(D13), 4160, doi:10.1029/2000JD000249, 2002.
- Wagner, C. F., Determination of the wave front of lightning stroke currents from field measurements, *Trans. Am. Inst. Electron. Eng., Part 3*, *79*, 581–589, 1960.
- Wagner, C. F., and A. R. Hileman, The lightning stroke, *Trans Am. Inst. Electron. Eng., Part 3*, *77*, 229–242, 1958.
- Wang, D., V. A. Rakov, M. A. Uman, N. Takagi, T. Watanabe, D. E. Crawford, K. J. Rambo, G. H. Schnetzer, R. J. Fisher, and Z. I. Kawasaki, Attachment process in rocket-triggered lightning strokes, *J. Geophys. Res.*, *104*, 2143–2150, 1999.
- Weidman, C. D., and E. P. Krider, The fine structure of lightning return stroke wave forms, *J. Geophys. Res.*, *83*, 6239–6247, 1978.
- Weidman, C. D., and E. P. Krider, Submicrosecond risetimes in lightning return-stroke fields, *Geophys. Res. Lett.*, *7*, 955–958, 1980.
- Willett, J. C., V. P. Idone, R. E. Orville, C. Leteinturier, A. Eybert-Berard, L. Barret, and E. P. Krider, An experimental test of the “transmission-line model” of the electromagnetic radiation from triggered lightning return strokes, *J. Geophys. Res.*, *93*, 3867–3878, 1988.
- Willett, J. C., J. C. Bailey, V. P. Idone, A. Eybert-Berard, and L. Barret, Submicrosecond intercomparison of radiation fields and currents in triggered lightning return strokes based on the “transmission-line model,” *J. Geophys. Res.*, *94*, 13,275–13,286, 1989.

---

J. Jerauld, V. A. Rakov, K. J. Rambo, G. H. Schnetzer, J. Schoene, and M. A. Uman, Department of Electrical and Computer Engineering, University of Florida, 311 Larsen Hall, Gainesville, FL 32611, USA. (jjerauld@ufl.edu; rakov@ece.ufl.edu; rambo@tec.ufl.edu; gschnetzer@zianet.com; jenss@ufl.edu; uman@ece.ufl.edu)